frontiers | Frontiers in Chemistry

TYPE Original Research
PUBLISHED 17 March 2025
DOI 10.3389/fchem.2025.1558075

OPEN ACCESS

EDITED BY
Wei Li,
Toho University, Japan

REVIEWED BY
Bingyang Zhang,
Tianjin University of Traditional Chinese Medicine, China
Sagnik Sengupta,
University of Texas Southwestern Medical Center, United States

*CORRESPONDENCE
Jia Xu,
doctorxujia@163.com

†These authors have contributed equally to this work

RECEIVED 09 January 2025
ACCEPTED 19 February 2025
PUBLISHED 17 March 2025

CITATION
Shi Y-C, Yu Y-X, Gao J-X, Wang X, Shang X-Y and Xu J (2025) Iridoid glycoside dimers from fruits of *Cornus officinalis* and their anti-inflammatory activity.
Front. Chem. 13:1558075.
doi: 10.3389/fchem.2025.1558075

Iridoid glycoside dimers from fruits of *Cornus officinalis* and their anti-inflammatory activity

Ying-Chu Shi[1,2†], Yu-Xin Yu[1,2†], Jiu-Xia Gao[1,2], Xin Wang[3], Xiao-Ya Shang[3] and Jia Xu[2*]

[1]Beijing University of Chinese Medicine, Beijing, China, [2]Beijing Hospital of Traditional Chinese Medicine, Capital Medical University, Beijing, China, [3]College of Applied Arts and Science, Beijing Union University, Beijing, China

A bioassay-guided phytochemical study of the fruits of *Cornus officinalis* led to the isolation of six new iridoid glycoside dimers, named corndiridoside A-F (**1–6**), along with 11 analogs (**7–17**). The structure of these dimers was elucidated using HRESIMS, 1D and 2D NMR, IR, and UV spectra, as well as literature comparisons. The anti-inflammatory activity of all compounds was evaluated, revealing a significant inhibitory effect on all dimers on the production of NO in LPS-stimulated RAW 264.7 cells at concentrations of 25 and 50 μM. Of the six, compounds **2** and **3** showed the strongest anti-inflammatory activity.

KEYWORDS

***Cornus officinalis*, iridoid glycoside dimers, isolation, structure identification, anti-inflammatory activity**

1 Introduction

Inflammation is a defensive response of host tissues to injuries, external pathogens, and foreign bodies; long-term inflammatory responses and persistent chronic inflammation can damage the body's homeostasis (Kotas and Medzhitov, 2015). Inflammatory responses include both acute and chronic inflammation. Chronic inflammation is associated with diseases such as diabetes, obesity, cancer, atherosclerosis, neurological diseases, and atopic dermatitis (Headland and Norling, 2015; Germolec et al., 2018). Natural products with anti-inflammatory activity and extracted from plants play an important role in the development of anti-inflammatory drugs or functional foods.

Cornus officinalis plant belongs to the Cornaceae family and is mainly found in East Asia, including China, Korea, and Japan. Its dried mature fruits are widely used both as traditional Chinese medicine as well as healthy edible food and have anti-inflammatory, antioxidation, neuroprotective, and hypoglycemic effects (Huang et al., 2018; Gao et al., 2021). The extract of *C. officinalis* has shown significant anti-inflammatory activity in several studies (Sung et al., 2009; Quah et al., 2020; Yang et al., 2024). For example, Quanh et al. (2020) reported that the ethanol extract of *C. officinalis* had a potential therapeutic effect on atopic dermatitis by inhibiting iNOS mRNA expression, and pro-inflammatory cytokines (IL-1β, IL-6, and TNF-α) and LPS-induced nitric oxide (NO) production in RWA 264.7 cells (Quah et al., 2020). Iridoid glycosides, gallate derivatives, and triterpenoids are considered to be anti-inflammatory components of *C. officinalis* (Jang et al., 2014; Yuan et al., 2020; Li et al., 2021). Of these components, iridoid glycosides, including monomers and dimers, are the main anti-inflammatory active ingredients in *C. officinalis*. Total cornel iridoid glycoside and some iridoid glycosides including morroniside, loganin, cornuside, and iridoid dimers have been reported to show significant anti-inflammatory activity by

regulating different inflammatory factors (Ye et al., 2017; Park et al., 2021; Peng et al., 2022; Wang et al., 2022; Zheng et al., 2022; Tong et al., 2023; Yan et al., 2024). Although some iridoid glycosides with anti-inflammatory activity have been extracted from *C. officinalis*, their anti-inflammatory components remain poorly understood. To further elucidate the anti-inflammatory activity of iridoid glycosides, based on an *in vitro* anti-inflammatory activity test, the 50% ethanol aqueous extract of *C. officinalis* was chromatographically isolated to obtain the iridoid glycoside enrichment site with the strongest anti-inflammatory activity. Herein, six new iridoid glycoside dimers (**1–6**) and 11 (**7–17**) analogs were isolated from the strongest anti-inflammatory fraction, and their isolated procedures, and structural elucidation were reported in the present study. Additionally, the *in vitro* anti-inflammatory activity of the isolated compounds was measured on the LPS-stimulated RAW 264.7 cells model.

2 Materials and methods

2.1 General Experimental Procedures

Nuclear magnetic resonance (NMR) spectroscopy of isolated compounds (CD_3OD) was acquired on a Bruker AV-III-500 (500 MHz for ^1H and 125 MHz for ^{13}C) spectrometers (Bruker, Billerica, MA, United States). High-resolution electrospray ionization mass spectroscopy (HRESIMS) data were obtained using a Thermo QE Plus spectrometer (Thermo Scientific, Waltham, MA, United States). Optical rotation data were recorded using a Rudolph Research Autopol III automatic polar spectrometer (Rudolph Research Analytical, Zurich, Switzerland). Infrared (IR) spectra were recorded on a Nicolet Impact 400 FT-IR spectrophotometer (Nicolet, Madison, WI, United States). Furthermore, column chromatographical separation was performed on Diaion HP-20 macroporous resin (Mitsubishi Chemical Corporation, Tokyo, Japan), Sephadex LH-20 gel (Pharmacia Biotech AB, Uppsala, Sweden), silica gel (Qingdao Marin Chemical Inc., Qingdao, China). A Waters HPLC (Waters 2,545 controller with a Waters 2,998 dual-wavelength absorbance detector) with a Waters preparative Rp C_{18} chromatographic column (X-bridge, 250 mm × 19 mm, 5 μm) was employed for HPLC preparative (Waters, Milford, MA, United States). The chemical reagents, including analytical grade and chromatographic grade, were purchased from Tianjin Fuyu (Tianjin, China). The RAW 264.7 cells (No. 1101MOU-PUMC000146) used in this study were obtained from the National Infrastructure of Cell Line Resource (Peking Union Medical College, Beijing, China).

2.2 Plant material

The matured and dried fruits of *C. officinalis* were obtained in June 2023 from the Beijing Hospital of Traditional Chinese Medicine (Beijing, China), and authenticated by Pro. Sheng Lin (Beijing University of Traditional Chinese Medicine). A voucher specimen (No. 20230101) has been deposited at the Department of Dermatology, Beijing Hospital of Traditional Chinese Medicine, Beijing, China.

2.3 Isolation and purification

The air-dried fruits (10 kg) of *C. officinalis* were powdered and extracted with 50% EtOH aqueous (100 L × 3) by ultrasound at room temperature. After filtration, the extract was evaporated under reduced pressure to obtain crude extract. After suspending into H_2O, a Diaion HP-20 Macroporous Resin column was used to separate the extract with EtOH-H_2O (0:100, 20:80, 40:60, 70:30, and 95:5, *v/v*), yielding five fractions (Fr.A –Fr. E). The EtOH-H_2O (40:60) fraction (Fr. C) was further subjected to a silica gel chromatography eluting with $CHCl_3$-MeOH (15:1 – 8:1, *v/v*) to afford six major fractions (Fr.C1 – Fr.C6). The anti-inflammatory activity test exhibited that Fr.C4 had the strongest inhibitory activity; therefore, it was selected as the target fraction for further separation. Fraction Fr.C4 was subjected to a reversed-phase C_{18} silica gel with MeOH-H_2O (10:90 – 100:0, *v/v*) to obtain seven faction Fr.C4-1 ~ Fr.C4-7. Subfraction Fr.C4-2 was further separated by a reversed-phase C_{18} silica gel eluting with MeOH-H_2O (20:80 ~ 100:0, *v/v*) to yield five fractions Fr.C4-2-1~ Fr.C4-2-5. Subfraction Fr.C4-2-2 was separated by a Sephadex LH-20 gel column ($CHCl_3$-MeOH 2:1, *v/v*) and further purified by preparative HPLC using MeCN-H_2O (20:80, 18 mL/min) to yield compounds **7**, **9**, and **12**. Subfraction Fr.C4-2-3 was subjected to a Sephadex LH-20 gel column eluting with $CHCl_3$-MeOH (2:1, *v/v*) and further purified by preparative HPLC eluting with MeOH-H_2O (40:60, 18 mL/min) to yield **4**, **14** and **8**. Fr.C4-2-4 was purified using preparative HPLC eluting with MeCN-H_2O (20:80, 18 mL/min) to yield compounds **5** and **6**. Subfraction Fr.C4-2-5 was given to a Sephadex LH-20 gel column eluting with $CHCl_3$-MeOH (2:1, *v/v*) and further purified by using preparative HPLC (20% MeCN/H_2O, 18 mL/min) to yield **1**, **10** and **11**. Fr.C4-3 was purified on a Sephadex LH-20 gel column with $CHCl_3$-MeOH (2:1, *v/v*) elution and further prepared by HPLC (20% MeCN/H_2O, 18 mL/min) to yield compounds **13** and **15**. Fr.C4-4 was given to HPLC using 40% MeOH/H_2O (18 mL/min) to yield **16** and **17**. Fr.C4-6 was separated on a Sephadex LH-20 gel column with $CHCl_3$-MeOH (2:1, *v/v*) and further purified by using preparative HPLC (25% MeCN/H_2O, 18 mL/min) to yield compounds **2** and **3**.

Corndiridoside A (**1**): White amorphous powder; [α] −45.6 (0.03, MeOH); UV (MeOH) λ_{max} (log ε) 239 (3.95) nm; IR ν_{max} 3,401, 2,916, 1703, 1,636, 1,077 cm^{-1}; ^1H NMR (500 MHz, CD_3OD) and ^{13}C NMR (125 MHz, CD_3OD) (see Table 1); HRESIMS *m/z* 775.26660 $[M-H]^-$ (calculated for $C_{34}H_{47}O_{20}$, 775.26662).

Corndiridoside B (**2**) White amorphous powder; [α] −65.6 (0.02, MeOH); UV (MeOH) λ_{max} (log ε) 238 (4.00), 282 (3.24) nm; IR ν_{max} 3,392, 2,939, 1,682, 1,639, 1,078 cm^{-1}; ^1H NMR (500 MHz, CD_3OD) and ^{13}C NMR (125 MHz, CD_3OD) see Table 1; HRESIMS *m/z* 901.29828 $[M-H]^-$ (calculated for $C_{40}H_{53}O_{23}$, 901.29831).

Corndiridoside C (**3**) White amorphous powder; [α] −63.1 (0.02, MeOH); UV (MeOH) λ_{max} (log ε) 238 (4.01), 282 (3.13) nm; IR ν_{max} 3,424, 2,906, 1,681, 1,639, 1,076 cm^{-1}; ^1H NMR (500 MHz, CD_3OD) and ^{13}C NMR (125 MHz, CD_3OD) see Table 1; HRESIMS *m/z* 901.29816 $[M-H]^-$ (calculated for $C_{40}H_{53}O_{23}$, 901.29831).

10.3389/fchem.2025.1558075

TABLE 1 The ^{1}H and^{13}C NMR data of compounds 1–3.

Position	1		2		3	
	δ_H	δ_C	δ_H	δ_C	δ_H	δ_C
1	5.66, d, *J* = 2.8 Hz	94.9	5.90, d, *J* = 9.3 Hz	95.8	5.82, d, *J* = 8.8 Hz	96.1
3	7.51, d, *J* = 1.1 Hz	153.2	7.52, s	154.5	7.55, s	154.1
4	—	111.1	—	111.7	—	110.8
5	3.29, m	28.1	3.06, m	27.8	2.81, m	31.8
6	(a) 2.55, m (b) 2.61, dd, *J* = 19.1, 11.2 Hz	43.4	(a) 1.45, m (b) 1.97, m	34.0	(a) 1.14, m (b) 1.96, m	35.7
7	—	220.8	4.92, d, *J* = 3.2 Hz	99.1	5.00, d, *J* = 3.2 Hz	102.4
8	2.09, m	44.5	4.41, m	66.5	3.92, m	74.1
9	2.34, m	46.5	1.81, m	40.3	1.84, m	40.3
10	1.15, d, *J* = 7.1 Hz	13.5	1.34, d, *J* = 6.9 Hz	19.7	1.40, d, *J* = 6.9 Hz	19.7
11	—	168.9	—	168.6	—	168.6
12	3.71, s	51.8	3.67, s	51.7	3.66, s	51.7
Glc-1′	4.75, d, *J* = 7.8 Hz	99.7	4.81, d, *J* = 7.9 Hz	100.4	4.83, *J* = 7.3 Hz	100.2
2′	3.21, m	73.2	3.34, m	75.0	3.41, m	75.2
3′	3.59, m	86.0	3.28, m	78.5	3.30, m	78.4
4′	3.38, m	70.2	3.36, m	71.6	3.38, m	72.2
5′	3.27, m	78.2	3.48, m	76.7	3.51, m	77.2
6′	(a) 3.66, dd, *J* = 5.6, 11.9 Hz (b) 3.90, dd, *J* = 1.5, 11.9, Hz	62.9	(a) 3.62, dd, *J* = 1.9, 11.2 Hz (b) 3.97, dd, *J* = 6.1, 11.2 Hz	67.6	(a) 3.6, dd, *J* = 7.5, 11.5 Hz (b) 4.03, dd, *J* = 1.7, 11.5 Hz	68.5
1″	5.88, d, *J* = 9.3 Hz	96.4	5.84, d, *J* = 9.3 Hz	95.7	5.78, d (8.8)	95.6
3″	7.52, s	154.7	7.51, s	154.6	7.43, s	154.5
4″	—	110.8	—	111.7	—	111.7
5″	2.87, m	32.1	3.06, m	27.8	3.09, m	27.8
6″	(a) 1.31, m (b) 2.25, m	35.5	(a) 1.40, m (b) 1.90, m	33.7	(a) 1.51, m (b) 1.99, m	34.0
7″	4.79, dd, *J* = 2.3, 9.6 Hz	103.3	4.87, d, *J* = 3.2 Hz	97.9	4.80, d, *J* = 3.0 Hz	99.7
8″	4.01, m	74.4	4.30, m	66.3	4.45, m	66.5
9″	1.81, m	39.8	1.81, m	40.1	1.79, m	40.0
10″	1.45, d, *J* = 6.8 Hz	19.7	1.25, d, *J* = 6.85 Hz	19.6	1.36, d, *J* = 6.9 Hz	19.7
11″	—	168.6	—	168.6	—	168.6
12″	3.70, s	51.7	3.68, s	51.7	3.70, s	51.7
Glc-1‴	4.75, d, *J* = 7.8 Hz	100.7	4.80, d, *J* = 7.9 Hz	100.0	4.80, d, *J* = 7.9 Hz	100.1
2‴	3.19, m	74.9	3.24, m	75.0	3.22, m	75.0
3‴	3.21, m	78.7	3.26, m	78.1	3.30, m	78.0
4‴	3.24, m	71.8	3.26, m	71.7	3.30, m	71.5
5‴	3.36, m	78.0	3.38, m	77.9	3.40, m	77.9
6‴	(a) 3.55, dd, *J* = 12.3, 6.7 Hz (b) 3.85, dd, *J* = 12.3, 1.9 Hz	62.5	(a) 3.67, m (b) 3.89, dd, *J* = 1.8, 11.1 Hz	62.8	(a) 3.67, m (b) 3.87, dd,*J* = 1.9, 12.2 Hz	62.8
1⁗			9.56	179.5	9.58	179.6

(Continued on following page)

TABLE 1 (*Continued*) The ^{1}H and^{13}C NMR data of compounds 1–3.

Position	1		2		3	
	δ_H	δ_C	δ_H	δ_C	δ_H	δ_C
2‴″			—	154.2	—	154.6
3‴″			6.67, d, *J* = 3.5 Hz	124.9	6.64, d, *J* = 3.6 Hz	124.0
4‴″			7.38, d, *J* = 3.5 Hz	112.9	7.41, d, *J* = 3.6 Hz	112.7
5‴″			—	160.0	—	159.8
6‴″			4.59, d, *J* = 13.7 Hz 4.63, d, *J* = 13.7 Hz	61.9	4.64, d, *J* = 13.8 Hz 4.64, dd, *J* = 1.6, 13.8 Hz	63.2

Recorded at 500 MHz (^{1}H NMR) and 125 MHz (^{13}C NMR) in CD_3OD.

Corndiridoside D (**4**) White amorphous powder; [α] −35.6 (0.03, MeOH); UV (MeOH) λ_{max} (log ε) 243 (4.00) nm; IR ν_{max} 3,418, 2,922, 1,693, 1,616, 1,077 cm^{-1}; ^{1}H NMR (500 MHz, CD_3OD) and ^{13}C NMR (125 MHz, CD_3OD) see Table 2; HRESIMS *m/z* 745.25659 $[M-H]^-$ (calculated for $C_{33}H_{45}O_{19}$, 745.25605).

Corndiridoside E (**5**) White amorphous powder; [α] −27.4 (0.02, MeOH); UV (MeOH) λ_{max} (log ε) 244 (4.20) nm; IR ν_{max} 3,393, 2,912, 1,696, 1,617, 1,074 cm^{-1}; ^{1}H NMR (500 MHz, CD_3OD) and ^{13}C NMR (125 MHz, CD_3OD) see Table 2; HRESIMS *m/z* 745.25513 $[M-H]^-$ (calculated for $C_{33}H_{45}O_{19}$, 745.25605).

Corndiridoside F (**6**) White amorphous powder [α] −31.6 (0.02, MeOH); UV (MeOH) λ_{max} (log ε) 239 (4.20) nm; IR ν_{max} 3,403, 2,927, 1,697, 1,618, 1,074 cm^{-1}; ^{1}H NMR (500 MHz, CD_3OD) and ^{13}C NMR (125 MHz, CD_3OD) see Table 2; HRESIMS *m/z* 745.25549 $[M-H]^-$ (calculated for $C_{33}H_{45}O_{19}$, 745.25605).

2.4 Acid hydrolysis and determination of the stereochemistry of the sugar moiety of 1–6

The acid hydrolysis method of each compound has previously been reported (Wang et al., 2018). Each compound (**1–6,** 1.0 mg) was dissolved in 2 M HCl (2.0 mL) and reacted at 80°C for 1.5 h. EtOAc was used to extract the reaction mixture and obtain an H_2O layer. After evaporation and dilution by H_2O, a neutral residue was obtained. Then, anhydrous pyridine (1.0 mL) and 1 mg of L-cysteine methyl ester hydrochloride was added. After stirring at 60°C for 2 h, the mixture was evaporated to dryness, and 0.1 mL of N-trimethylsilyl imidazole was added. After stirring 2 h at 60°C, the reaction mixture was extracted with n-hexane. The n-hexane extract was subjected to GC analysis with an HP-5 capillary column (30 m, 0.25 mm, Dikma), FID detection, 280°C detector temperature, and a stepwise heating from 160°C to 280°C at 5°C/min, using N_2 as the carrier gas. Compared with the retention time of D-glucose (20.55 min), the sugar of all compounds was found to be D-glucose.

2.5 Anti-inflammatory activity test in LPS-stimulated RAW264.7 cells

The anti-inflammatory activity of the isolated compounds was determined by a previously reported method (Xu et al., 2024). The cell viability assay was measured using CCK-8 assay and NO production in LPS-stimulated RAW264.7 cells was measured using Griess assay. All experiments were performed in triplicate. Data were processed using GraphPad Prism 9.0.

3 Results and discussion

3.1 Structure elucidation

Guided by the anti-inflammatory activity test, six new iridoid glycoside dimers (**1–6**) and eleven known iridoid glycoside dimers (**11–17**) were isolated from the fraction with strong anti-inflammatory activity using chromatography techniques (Figure 1).

Compound **1** was obtained as an amorphous white powder. HRESIMS data exhibited an ion at *m/z* 775.26660 $[M-H]^-$, confirming the molecular formula to be $C_{34}H_{48}O_{20}$ with an unsaturation of 11. The IR spectra had absorption bands at 3,401 cm^{-1} (hydroxyl group), 1737 and 1703 cm^{-1} (carbonyl groups). The ^{1}H NMR data (Table 1) of compound **1** displayed two olefinic protons at δ_H 7.52 (1H, s, H-3″) and 7.51 (1H, d, *J* = 1.1 Hz, H-3), four oxygenated methine protons at δ_H 5.66 (1H, d, *J* = 2.8 Hz, H-1), 5.88 (1H, d, *J* = 9.3 Hz, H-1″), 4.79 (1H, dd, *J* = 9.6, 2.3 Hz, H-6″), and 4.01 (1H, m, H-8″), two methoxy protons at δ_H 3.71 (3H, s, H-12) and 3.70 (3H, s, H-12″), and a series of glycosyl protons. The molecular formula and ^{13}C NMR data suggested that structure **1** could be an iridoid dimer. ^{13}C NMR data combined with HSQC spectrum suggested the presence of one ketone carbonyl carbon signal (δ_C 220.8), two ester carbonyl carbon signals (168.6 and 168.9), four olefin carbon signals (δ_C 111.1, 153.2, 110.8, 154.7), two methoxy carbon signals (δ_C 51.8 and 51.7), two secondary methyl carbon signals (δ_C 13.5 and 19.7), five acetal carbon signals (δ_C 94.9, 96.4, 99.7, 100.7, 103.3) and one oxygenated methine carbon signal (δ_C 74.4). A series of signals for two glycosyl compounds were displayed at δ_C 86.0, 78.7, 78.2, 78.0, 74.9, 73.2, 71.8, 70.2, 62.9, and 62.5. A comparison of the data for **1** with those of 7*α*-morroniside (Han et al., 2004) and 7-dehydrologanin (Chen et al., 2017) suggested that **1** might be a condensation product of the above two compounds.

Comprehensive analysis of the two dimensional NMR (2D NMR) data displayed the planar structure of **1** (Figure 1). ^{1}H-^{1}H COSY spectrum demonstrated the spin system involving C6-C5-C9-C1 and C8-C9, combined with the HMBC correlations from H-5 to C-7, from H-10 to C-9 and C-7, from H-1 to C-3, C-5 and C-1″, from H-6 to C-4, from H-3 to C-11, and from H-12 to C-11 indicated the presence of a 7-dehydrologanin unit (Figure 2).

10.3389/fchem.2025.1558075

TABLE 2 ^{1}H and^{13}C NMR data of compounds 4–6

Position	4		5		6	
	δ_H	δ_C	δ_H	δ_C	δ_H	δ_C
1	5.56, d, *J* = 1.7 Hz	97.6	5.57, d, *J* = 1.4 Hz	98.0	5.50, d, *J* = 1.7 Hz	98.0
3	7.61, d, *J* = 2.4 Hz	153.8	7.61, d, *J* = 2.4 Hz	154.0	7.59, d, *J* = 2.4 Hz	153.9
4	—	106.2	—	105.9	—	106.0
5	3.15, m	28.4	3.13, m	28.5	3.14, m	28.4
6	(a) 1.69, m (b) 1.77, m	25.9	(a) 1.73, m (b) 1.83, m	25.9	(a) 1.69, m (b) 1.77, m	25.9
7	(a) 4.44, m (b) 4.46, m	69.8	(a) 4.38, m (b) 4.46, m	69.6	(a) 4.38, td, *J* = 2.4, 11.7 Hz (b) 4.46, m	69.7
8	5.53, m	133.3	5.56, m	133.5	5.55, m	133.3
9	2.69, m	43.7	2.70, m	44.0	2.70, m	43.8
10	5.29, m	120.8	5.30, dd, *J* = 1.7, 10.4 Hz 5.34, dd, *J* = 1.5, 17.3 Hz	120.9	5.29, m	120.8
11	—	168.7		168.5	—	168.4
12	—	—	—	—	—	—
Glc-1′	4.77, d, *J* = 7.9 Hz	99.1	4.71, d, *J* = 8.0 Hz	99.6	4.67, d, *J* = 7.9 Hz	99.7
2′	3.38, m	73.2	3.23, m	75.4	3.21, m	74.8
3′	3.60, m	85.7	3.55, t, *J* = 8.7 Hz	83.1	3.50, t, *J* = 9.1 Hz	77.4
4′	3.19, m	70.1	3.37, m	70.1	3.59, t, *J* = 9.4 Hz	76.6
5′	3.36, m	78.1	3.40, m	78.0	3.34, m	76.9
6′	(a) 3.56, m (b) 3.83, dd, *J* = 1.7, 11.9 Hz	63.0	(a) 3.67, m (b) 3.90, m	62.8	(a) 3.80, dd, *J* = 4.8, 12.6 Hz (b) 3.88, m	63.3
1″	5.87, d, *J* = 9.4 Hz	96.5	5.90, d, *J* = 9.2 Hz	95.6	5.88, d, *J* = 9.4 Hz	96.0
3″	7.52, s	154.7	7.54, s	154.6	7.52, s	154.5
4″	—	110.8	—	111.7	—	110.7
5″	2.87, m	32.1	3.11, m	27.6	2.82, m	32.0
6″	(a) 1.32, m (b) 2.29, m	35.5	(a) 1.53, m (b) 2.05, m	34.0	(a) 1.23, m (b) 2.20, m	35.6
7″	4.80, d, *J* = 2.3 Hz	103.0	5.34, d, *J* = 3.6 Hz	99.0	4.93, d, *J* = 2.2 Hz	103.5
8″	4.01, m	74.4	4.73, m	66.5	3.92, m	74.1
9″	1.81, m	39.7	1.82, m	40.5	1.79, m	39.8
10″	1.46, d, *J* = 6.8 Hz	19.7	1.32, d, *J* = 6.9 Hz	19.5	1.43, d, *J* = 6.8 Hz	19.7
11″	—	168.5	—	168.8	—	168.6
12″	3.70, s	51.7	3.71, s	51.73	3.70, s	51.7
Glc-1‴	4.74, d, *J* = 7.8 Hz	100.8	4.80, *J* = 7.9 Hz	100.0	4.77, d, *J* = 7.8 Hz	100.3
2‴	3.22, m	74.9	3.23, m	75.0	3.22, m	75.0
3‴	3.27, m	78.9	3.39, m	78.5	3.21, m	78.4
4‴	3.20, m	71.7	3.29, m	71.6	3.30, m	71.4
5‴	3.35, m	77.9	3.30, m	78.3	3.36, m	77.9
6‴	(a) 3.67, m (b) 3.89, dd, *J* = 1.8 12.1 Hz	62.4	(a) 3.70, m (b) 3.92, m	62.9	(a) 3.70, m (b) 3.89, m	62.6

The 1H NMR of compounds 1-6 were recorded at 500 MHz (^{1}H NMR) and 125 MHz (^{13}C NMR) in CD_3OD.

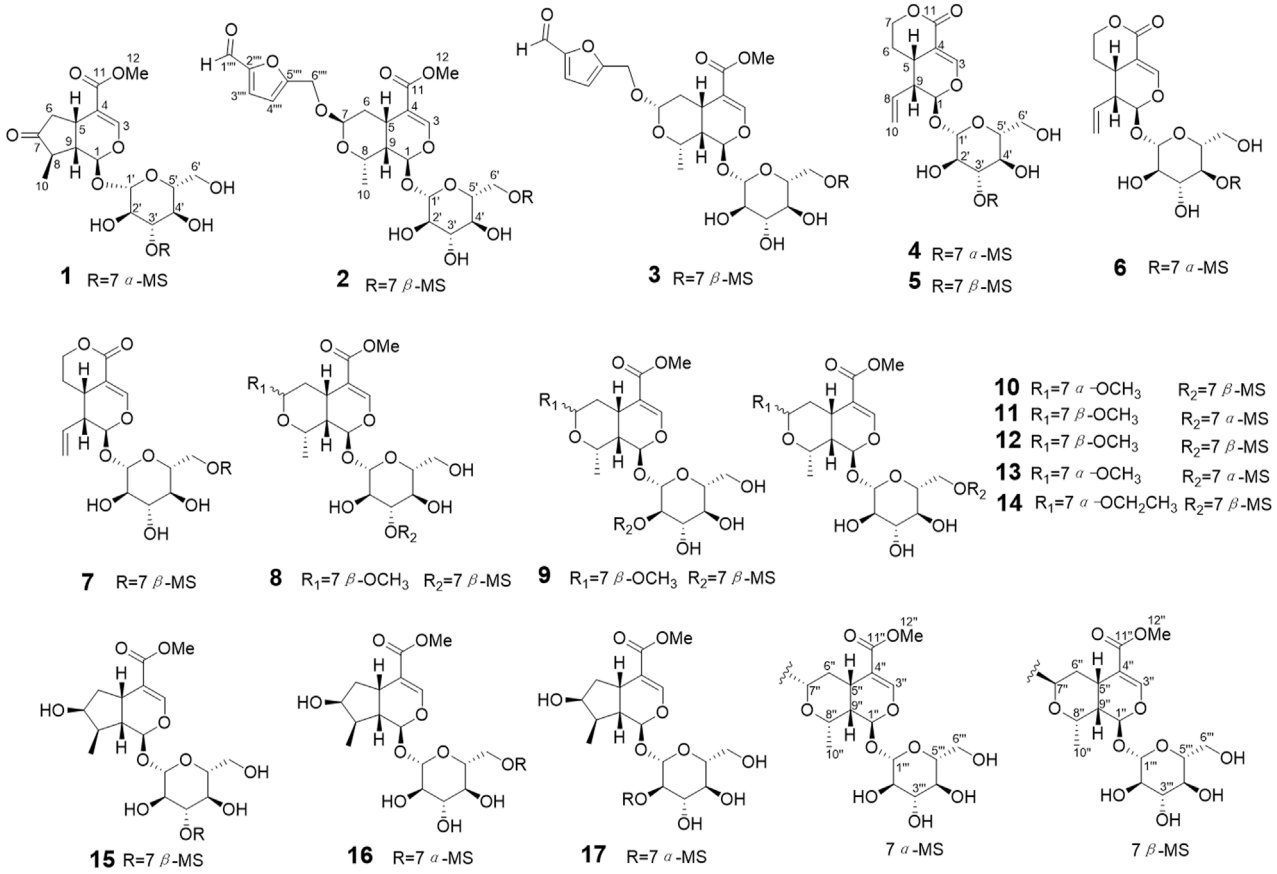

FIGURE 1
The structures of compounds **1**–**17**.

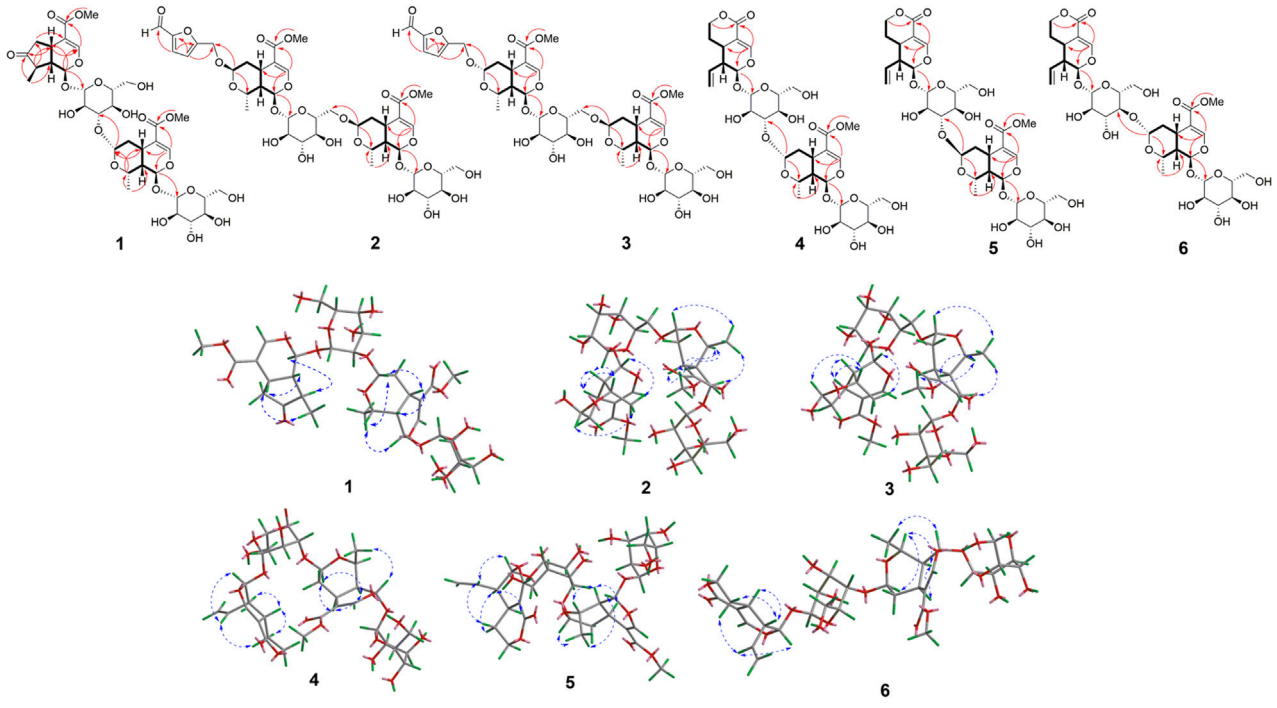

FIGURE 2
The ^{1}H-^{1}H COSY (▬) HMBC ( ) and NOESY ( ) correlations of compounds **1**–**6**.

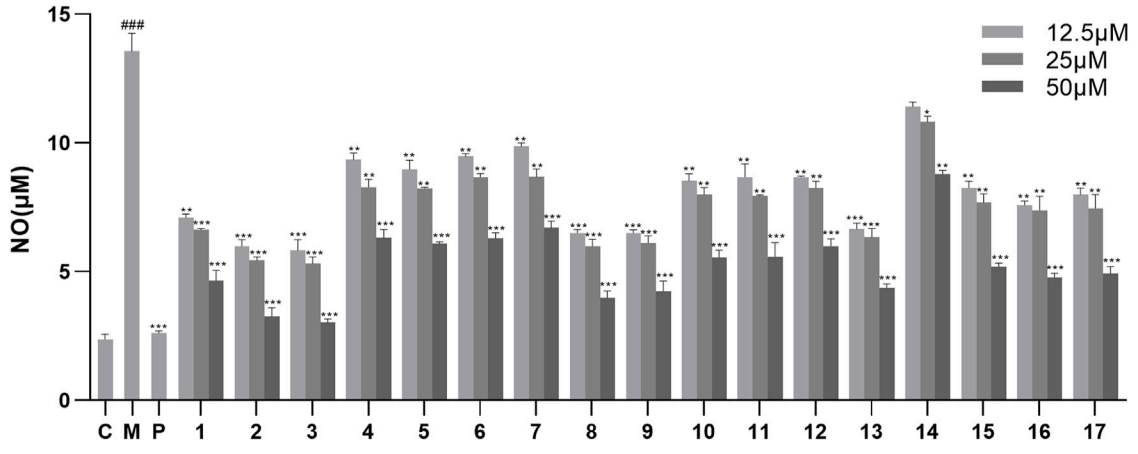

FIGURE 3
Effects of NO production in LPS-stimulated RAW246.7 cells treated with compounds **1–17**. Data are expressed as mean ± S. D (n = 3). C = control, M = model, P = hydrocortisone. *p < 0.05, **p < 0.01 and ***p < 0.001 vs. LPS-simulated group, ###p < 0.001 vs. control group.

Additionally, ^{1}H-^{1}H COSY correlations of H-1′′/H-9″, H-9′′/H-8″, H-9′′/H-5″, H-5′′/H-6″ combined with HMBC correlations from H-8″ to C-5″ and C-7″, from H-7″ to C-5″, H-3″ to C-5″ and C-1‴ established the 7*α*-morroniside unit. The key HMBC correlations of H-7″ with C-3′ suggested the linkage of C-7″-O-C-3′. The ROESY spectra exhibited correlations of H-1/H-8, H-1′′/H-10″, suggesting H-1, H-8, H-1″, and H-10″ were co-facial and defined as *α*-orientation (Figure 2). Consequently, ROESY correlations of H-10/H-5, H-5/H-9, H-8′′/H-7′′/H-5″, H-5′′/H-9″ indicated the H-5, H-9, H-10, H-5″, H-7″, H-8″ and H-9″ were in *β*-oriented. Based on the fact that iridoid compounds in *C. officinalis* are all 5*β* and 9*β* configurations, according to the coupling constants and chemical shifts of H-1, H-1″, H-7″, the absolute configurations of C-1, C-1″, and C-7 were determined to be 1*R*, 1″*R* and 7″*S*. Furthermore, the configurations of C-1, C-5, C-8, C-9, C-1″, C-5″, C-7″, C-8″ and C-9″ were identified as 1*R*, 5*S*, 8*R*, 9*S*, 1″*R*, 5″*S*, 7″*S*, 8″*S* and 9″*S*, which were consistent with 7*α*-morroniside (Han et al., 2004) and 7-dehydrologanin (Chen et al., 2017). After acid hydroxylation and derivatization, **1** was confirmed as D-glucose by GC analysis. The coupling constants of the anomeric proton signal at δ_H 4.75 (1H, d, *J* = 7.8 Hz, H-1′) and 4.76 (1H, d, *J* = 7.8 Hz, H-1‴) confirmed the *β*-configuration of D-glucose. Compound **1** was assigned as corndiridoside A.

Compound **2** was obtained as an amorphous powder with the molecular formula $C_{40}H_{54}O_{23}$ by HRESIMS *m/z* 901.29828 [M-H]$^-$ analysis. Its ^{1}H NMR displayed four olefin protons at δ_H 6.67 (1H, d, *J* = 3.5 Hz, H-3′′′′), 7.38 (1H, d, *J* = 3.5 Hz, H-4′′′′), 7.51 (1H, s, H-3″), and 7.52 (1H, s, H-3), six acetal protons at δ_H 4.80 (1H, d, *J* = 7.9 Hz, H-1‴), 4.81 (1H, *J* = 7.9 Hz, H-1′), 4.87 (1H, d, *J* = 3.2 Hz, H-7″), 4.92 (1H, d, *J* = 3.2 Hz, H-7), 5.84 (1H, d, *J* = 9.3 Hz, H-1″), and 5.90 (1H, d, *J* = 9.3 Hz, H-1). There are two oxygenated methine protons at δ_H 4.30 (1H, m, H-8″) and 4.41 (1H, m, H-8), and oxygenated methylene protons at δ_H 4.59 (1H, d, *J* = 13.7 Hz, H-6a′′′′) and 4.63 (1H, d, *J* = 13.7 Hz, H-6b′′′′); a series of protons displayed between δ_H 3.24 ~ 3.97 correspond to the sugar moieties. The ^{13}C NMR data showed 40 carbon signals, including two carbonyl carbon signals at δ_C 168.6 and 168.6, one ketone carbonyl carbon signals at δ_C 179.5, eight olefin carbon signals at δ_C 111.7, 111.7, 112.9, 124.9, 154.2, 154.5, 154.6, and 160.0, six acetal carbon signals at δ_C 95.7, 95.8, 97.9, 99.1, 100.0, and 100.4, two oxygenated methine carbon signals at δ_C 62.8 and 66.3, one oxygenated methylene carbon signal at δ_C 61.9, two methoxy carbon signals at δ_C 51.7. These NMR data showed close similarity to those of 7*β*-morroniside (Han et al., 2004). Combined with the molecular formula, **2** was speculated as a 7*β*-morroniside dimer with a 5-hydroxymethylfurfuraly moiety. The planar structure of **2** (Figure 1) was confirmed by the comprehensive analysis of the 2D NMR data (Figure 2). The key HMBC correlations of H-7″ with C-6′ indicated linkage of C-6′-O-C-7″ between two 7*β*-morroniside moieties. The structure of 5-hydroxymethylfurfuraly moiety was determined by the key HMBC correlations of H-3′′′′ with C-1′′′′ and C-5′′′′, H-4′′′′ with C-2′′′′ and C-6′′′′, which was connected to 7*β*-morroniside through 7-O-C-6′′′′ according to the HMBC correlations of H-7 with C-6′′′′. The configuration was found similar to that of the 7*β*-morroniside moieties by the NOESY correlations analysis as shown in Figure 2 and consistent with 7*β*-morroniside. Thus, compound **2** was determined as corndiridoside B.

Compound **3** had the same molecular formula as **2** according to HREISMS (*m/z* 901.29816 [M-H]$^-$) and NMR data (Table 1). The NMR spectrum of compound **3** was highly similar to that of **2**, except for the chemical downshift of C-7″ and C-8′′ (from δ_C 99.1, 66.5 to δ_C 102.4, 74.1), which indicated that one of the 7*β*-morroniside in **2** was replaced by 7*α*-morroniside in **3**. HMBC correlation of H-7″ with C-6′ confirmed that 7*α*-morroniside and 7*β*-morroniside were connected through C-6′-O-C-7″ bond (Figure 2). The HMBC correlation of H-7 with C-6′′′′ indicated that the 5-hydroxymethylfurfural moiety was linked to 7*α*-morroniside via an ester bond. Furthermore, the NOESY correlation between H-7″ and H-8*β* confirmed that H-7 was the *β*-oriented, and the absolute configuration was the same as 7*α*-morroniside and 7*β*-morroniside; hydrolysis and GC analysis proved that the sugar groups were D-glucose, so compound **3** was identified as corndiridoside C.

Compound **4** was a white amorphous powder. The molecular formula of $C_{33}H_{46}O_{19}$ was determined by the HRESIMS ion at *m/z*: 745.25659 [M−H]$^-$. The ^{1}H NMR data of **4** (Table 2) showed two four olefin protons, including two terminal olefinic protons at δ_H 5.53 (1H, m, H-8) and 5.29 (2H, m, H-10) and two olefin protons at

δ_H 7.52 (1H, s, H-3″), 7.61 (1H, d, J = 2.4 Hz, H-3), five acetal protons at δ_H 5.87 (1H, d, J = 9.4 Hz, H-1″), 4.74 (1H, d, J = 7.8 Hz, H-1‴), 4.77 (1H, d, J = 7.9 Hz, H-1′), 5.56 (1H, d, J = 1.7 Hz, H-1), 4.80 (1H, d, J = 2.3 Hz, H-7″), one oxygenated methylene proton at δ_H 4.44 (1H, m, H-7a) and 4.46 (1H, m, H-7b), one oxygenated methine proton at δ_H 4.01 (1H, m, H-8″), one methoxy protons at δ_H 3.70 (3H, s, H-12″), and a series of protons at δ_H 3.19 ~ 4.78 were assigned to the glycosyl groups. ^{13}C NMR and HSQC data were assigned to 33 carbon signals. Among them, there was one methyl carbon (δ_C 19.7), one methoxy carbon signal (δ_C 51.7), two oxygenated olefin carbon signals (δ_C 154.7, 153.8), four olefin carbon signals (δ_C 106.2, 110.8, 133.3, 120.8), five acetal carbon signals (δ_C 103.0, 96.5, 100.8, 97.6, 99.1), one oxygenated methylene carbon signal (δ_C 69.8), one oxygenated methine carbon signal (δ_C 74.4), two methylene carbon signals (δ_C 35.5 and 25.9), four methine carbon signals (δ_C 28.4, 43.7, 32.1, 39.7), two carbonyl carbon signals (δ_C 168.7 and 168.5), and two sets of glycosyl carbons (δ_C 62.4 ~ 100.8). The above data of **4** were very similar to those of 7α-morroniside (Han et al., 2004) and sweroside (Chen et al., 2017), indicating that **4** was an iridoid glycoside dimer. Detailed 2D NMR analysis confirmed the structures of the two moieties (Figure 2). In the ^{13}C NMR data of sweroside, the chemical shift of C-2′ was significantly shifted up (from δ_C 74.9 to 73.2) and the chemical shift of C-3′ was significantly shifted down (from δ_C 78.9 to 85.7), indicating that sweroside and 7α-morroniside were connected via C-3′-O-C-7″, which was also confirmed by the HMBC correlation from H-7″ to C-3′. The NOESY spectral correlations of H-8/H-1, H-8/H-6a, H-6b/H-5, H-6b/H-9, H-1‴/H-10″, H-8‴/H-5″, H-8‴/H-7″, H-5‴/H-7″ and H-5‴/H-9″, combined with chemical shift and coupling constants, thereby confirming the structure of compound **4**, which was named corndiridoside D.

Compound **5** has the molecular formula $C_{33}H_{46}O_{19}$ by the HRESIMS ion at m/z: 745.25513 $[M\text{-}H]^-$. Its NMR data (Table 2) was consistent with compound **4**, except for the obvious chemical upshift of C-7‴ (**4**, δ_C 103.0; **5**, δ_C 99.0 and C-8‴ (**4**, δ_C 74.4; **5**, δ_C 66.5) indicated the presence of 7β-morroniside unit in **5** instead of 7α-morroniside in **4**. The linkage of C-3′-O-C-7″ between two units was confirmed by the HMBC correlations of H-7″ and C-3′ (Figure 2). Compound **5** was determined as corndiridoside E.

Compound **6** has the same molecular formula of $C_{33}H_{46}O_{19}$ as compounds **4** and **5** based on the HREISMS (m/z: 745.25549 $[M\text{-}H]^-$) and NMR data (Table 2). The NMR data of **6** was very similar to those of **4,** except for the chemical shifts of C-3′, C-4′, and C-5′. The upshift of C-3′ (from δ_C 85.7 in **4** to δ_C 77.4 in **6**), C-5′ (from δ_C 78.1 in **4** to δ_C 76.9 in **6**) and downshift of C-4′ (from δ_C 70.1 in **4** to δ_C 76.6 in **6**) indicated that the 7α-morroniside moiety was linked via C-4′. HMBC correlation analysis of H-7″ at δ_H 4.93 and C-4′ at δ_C 76.6 confirmed that the C-7″ and C-4″ were lined via an ether bond (Figure 2). Thus, compound **6** was determined as corndiridoside F.

Comparing the NMR and HRESIMS data with literatures, 11 known compounds were identified as: cornuofficinaliside L (**7**) (Hao et al., 2023), cornuside C (**8**) (Ye et al., 2017), cornuside B (**9**) (Ye et al., 2017), cornuside E (**10**) (Ye et al., 2017), cornuside J (**11**) (Ye et al., 2017), cornuside A (**12**) (Ye et al., 2017), cornuside G (**13**) (Ye et al., 2017), cornuside K (**14**) (Ye et al., 2017), cornuofficinaliside D (**15**) (Hao et al., 2023), cornuside L (**16**) (Ye et al., 2017), cornuside M (**17**) (Ye et al., 2017).

3.2 Anti-inflammatory effects of compounds **1–17**

The inhibitory effects of the isolated compounds on NO production in LPS-stimulated RAW264.7 cells were evaluated. First, the cell viability assays exhibited that compounds **1–17** had no cytotoxic effect on RAW264.7 cells at a concentration below 50 μM (p > 0.05) (Supplementary Figure S1). Therefore, the inhibitory activity of compounds **1–17** on NO production in LPS-stimulated RAW264.7 cells was measured at concentrations of 12.5, 25, and 50 μM. As the results showed (Figure 3; Supplementary Table S1), compounds **1–17** showed significant anti-inflammatory activity at concentrations of 25 and 50 μM. Among them, compounds **2** and **3** exhibited the strongest anti-inflammatory activity in a dose-dependent manner, thereby suggesting that the 5-hydroxymethylfurfural group might enhance the activity. In addition, compound **14** showed the weakest anti-inflammatory activity compared with the other compounds, suggesting that the ethoxy group at the C-7 position might reduce its anti-inflammatory activity.

4 Conclusion

In summary, six new iridoid glycoside dimers, named corndiridoside A-F (**1–6**), and eleven known analogs (**7–17**) were isolated from the anti-inflammatory active fraction of *C. officinalis* fruits in the current study. The constituent units in these dimers are composed of morrnoiside, 7-dehydrologanin, and sweroside analogs. Among them, compound **1,** a dimer containing 7-dehydrologanin unit, was discovered for the first time from *C. officinalis*. In addition, their anti-inflammatory activities were assayed on the LPS-stimulated 264.7 RAW cell model. All compounds showed no cytotoxic effect on the cell viability of 264.7 RAW cells at 50 μM, and a majority of compounds exhibited significant anti-inflammatory activity at concentrations of 12.5, 25, and 50 μM. Compounds **2** and **3** containing 5-hydroxymethylfurfural group showed the strongest anti-inflammatory, indicating that the 5-hydroxymethylfurfural group might play an important role in enhancing anti-inflammatory activity. These compounds with anti-inflammatory activity may represent promising natural anti-inflammatory compounds that can be used in the development of drugs and functional foods. Moreover, this study also provides a basic scientific basis for the clinical anti-inflammatory application of *C. officinalis*.

Data availability statement

The original contributions presented in the study are included in the article/Supplementary Material, further inquiries can be directed to the corresponding author.

Author contributions

Y-CS: investigation, visualization, and writing–original draft. Y-XY: investigation, methodology, visualization, and

writing–original draft. J-XG: formal analysis, methodology, and writing–original draft. XW: investigation, methodology, visualization, and writing–original draft. X-YS: methodology and writing–review and editing. JX: conceptualization, funding acquisition, project administration, and writing–review and editing.

Funding

The author(s) declare that financial support was received for the research, authorship, and/or publication of this article. This work was financially supported by Capital's Funds for Health Improvement and Research (CFH) (No. 2024-3-7141).

Conflict of interest

The authors declare that the research was conducted in the absence of any commercial or financial relationships that could be construed as a potential conflict of interest.

Generative AI statement

The author(s) declare that no Generative AI was used in the creation of this manuscript.

Publisher's note

Supplementary material

The Supplementary Material for this article can be found online at: https://www.frontiersin.org/articles/10.3389/fchem.2025.1558075/full#supplementary-material

References

Chen, Y. J., Wang, Z. B., Yu, Y., Gao, Y., Yang, C. J., Bi, X. Y., et al. (2017). Structural identification of iridoids from leaves of *Hydrangea macrophylla*. *Chin. Tradit. Herb. Drugs* 48, 232–235. doi:10.7501/j.issn.0253-2670.2017.02.002

Gao, X., Liu, Y., An, Z., and Ni, J. (2021). Active components and pharmacological effects of *Cornus officinalis*: literature review. *Front. Pharmacol.* 12, 633447. doi:10.3389/fphar.2021.633447

Germolec, D. R., Shipkowski, K. A., Frawley, R. P., and Evans, E. (2018). Markers of inflammation. *Methods Mol. Biol.* 1803, 57–79. doi:10.1007/978-1-4939-8549-4_5

Han, S. Y., Pan, Y., Ding, G., and Cai, B. C. (2004). The ^{1}H-NMR and ^{13}C-NMR application in structural identification of iridoid compounds in *Cornus officinalis*. *Chin. Arch. Tradit. Chin. Med.* 24, 56. doi:10.13193/j.archtcm.2004.01.55.hanshy.028

Hao, Z. Y., Wang, X. L., Yang, M., Cao, B., Zeng, M. N., Zhou, S. Q., et al. (2023). Minor iridoid glycosides from the fruits of *Cornus officinalis* Sieb. et Zucc. and their anti-diabetic bioactivities. *Phytochemistry* 205, 113505. doi:10.1016/j.phytochem.2022.113505

Headland, S. E., and Norling, L. V. (2015). The resolution of inflammation: principles and challenges. *Semin. Immunol.* 27 (3), 149–160. doi:10.1016/j.smim.2015.03.014

Huang, J., Zhang, Y., Dong, L., Gao, Q., Yin, L., Quan, H., et al. (2018). Ethnopharmacology, phytochemistry, and pharmacology of *Cornus officinalis* Sieb. et Zucc. *J. Ethnopharmacol.* 213, 280–301. doi:10.1016/j.jep.2017.11.010

Jang, S. E., Jeong, J. J., Hyam, S. R., Han, M. J., and Kim, D. H. (2014). Ursolic acid isolated from the seed of *Cornus officinalis* ameliorates colitis in mice by inhibiting the binding of lipopolysaccharide to Toll-like receptor 4 on macrophages. *J. Agric. Food Chem.* 62 (40), 9711–9721. doi:10.1021/jf501487v

Kotas, M. E., and Medzhitov, R. (2015). Homeostasis, inflammation, and disease Susceptibility. *Cell* 160, 816–827. doi:10.1016/j.cell.2015.02.010

Li, H. B., Feng, Q. M., Zhang, L. X., Wang, J., Chi, J., Chen, S. Q., et al. (2021). Four new gallate derivatives from wine-processed *Corni* fructus and their anti-inflammatory activities. *Molecules* 26 (7), 1851. doi:10.3390/molecules26071851

Park, C., Lee, H., Kwon, C. Y., Kim, G. Y., Jeong, J. W., Kim, S. O., et al. (2021). Loganin inhibits lipopolysaccharide-induced inflammation and oxidative response through the activation of the Nrf2/HO-1 signaling pathway in RAW264.7 macrophages. *Biol. Pharm. Bull.* 44 (6), 875–883. doi:10.1248/bpb.b21-00176

Peng, Z., Wang, Y., He, J., Zhang, J., Pan, X., Ye, X., et al. (2022). Chemical constituents and their antioxidant and anti-inflammatory activities from edible *Cornus officinalis* fruits. *Eur. Food Res. Technol.* 248, 1003–1010. doi:10.1007/s00217-021-03940-6

Quah, Y., Lee, S. J., Lee, E. B., Birhanu, B. T., Ali, M. S., Abbas, M. A., et al. (2020). *Cornus officinalis* ethanolic extract with potential anti-allergic, anti-Inflammatory, and antioxidant activities. *Nutrients* 12 (11), 3317. doi:10.3390/nu12113317

Sung, Y. H., Chang, H. K., Kim, S. E., Kim, Y. M., Seo, J. H., Shin, M. C., et al. (2009). Anti-inflammatory and analgesic effects of the aqueous extract of *Corni fructus* in murine RAW 264.7 macrophage cells. *J. Med. Food* 12 (4), 788–795. doi:10.1089/jmf.2008.1011

Tong, Q., Xi, J., Cao, Y., He, R., Zhao, Y., Shao, Y., et al. (2023). Morroniside delays NAFLD progression in fructose-fed mice by normalizing lipid metabolism and inhibiting the inflammatory response. *J. Food Biochem.* 2023, 1–13. doi:10.1155/2023/9952583

Wang, X., Liu, C. H., Li, J. J., Zhang, B., Ji, L. L., and Shang, X. Y. (2018). Iridoid glycosides from the fruits of *Cornus officinalis*. *J. Asian. Nat. Prod. Res.* 20, 934–942. doi:10.1080/10286020.2018.1497609

Wang, X., Wu, Y., Wang, Z. Y., Li, J. J., Li, W., Li, Q., et al. (2022). Anti-inflammatory iridoid glycosides from fruits of *Cornus officinalis*. *Phytochem. Lett.* 52, 122–125. doi:10.1016/j.phytol.2022.10.006

Xu, Q. J., Liu, J. C., Huang, C. J., Wang, X., and Shang, X. Y. (2024). Seco-nortriterpenoids from *Cirsium setosum* and their anti-inflammatory activity. *Fitoterapia* 175, 105879. doi:10.1016/j.fitote.2024.105879

Yan, F., Wang, L., Zhang, J., Liu, Z., Yu, B., Li, W., et al. (2024). Cornuside alleviates psoriasis-like skin lesions in mice by relieving inflammatory effects. *Int. Immunopharmacol.* 134, 112183. doi:10.1016/j.intimp.2024.112183

Yang, H., Liu, H., Zheng, Y., Li, B., Wang, S., Zhang, J., et al. (2024). *Cornus Officinalis* total glycosides alleviate granulomatous lobular mastitis via the B7-CD28/CTLA-4 costimulatory pathway. *Chem. Biodivers.* 22, e202401539. doi:10.1002/cbdv.202401539

Ye, X. S., He, J., Cheng, Y. C., Zhang, L., Qiao, H. Y., Pan, X. G., et al. (2017). Cornusides A-O, bioactive iridoid glucoside dimers from the fruit of *Cornus officinalis*. *J. Nat. Prod.* 80 (12), 3103–3111. doi:10.1021/acs.jnatprod.6b01127

Yuan, J., Cheng, W., Zhang, G., Ma, Q., Li, X., Zhang, B., et al. (2020). Protective effects of iridoid glycosides on acute colitis via inhibition of the inflammatory response mediated by the STAT3/NF-κB pathway. *Int. Immunopharmacol.* 81, 106240. doi:10.1016/j.intimp.2020.106240

Zheng, C., Yang, C., Gao, D., Zhang, L., Li, Y., Li, L., et al. (2022). Cornel iridoid glycoside alleviates microglia-mediated inflammatory response via the NLRP3/Calpain pathway. *J. Agric. Food Chem.* 70 (38), 11967–11980. doi:10.1021/acs.jafc.2c03851